Gut and Liver
https://doi.org/10.5009/gnl210177
pISSN 1976-2283 eISSN 2005-1212

Original Article

Gut Microbiota Alteration Influences Colorectal Cancer Metastasis to the Liver by Remodeling the Liver Immune Microenvironment

Na Yuan[1,2,3], Xiaoyan Li[2], Meng Wang[4], Zhilin Zhang[3], Lu Qiao[2], Yamei Gao[2], Xinjian Xu[5], Jie Zhi[2], Yang Li[6], Zhongxin Li[7], and Yitao Jia[1,2]

[1]Department of Oncology, Hebei Medical University, [2]The Third Department of Oncology, Hebei General Hospital, Shijiazhuang, [3]Department of Radiotherapy, The First Affiliated Hospital of Hebei North University, Zhangjiakou, [4]Department of Clinical Psychology, Baoding No.1 Central Hospital, Baoding, [5]Department of Thoracic Surgery, The Fourth Hospital of Hebei Medical University, Shijiazhuang, [6]Department of Oncology, Affiliated Hospital of Hebei University, Baoding, and [7]Department of General Surgery, The First Hospital of Hebei Medical University, Shijiazhuang, China

Article Info
Received April 17, 2021
Revised October 12, 2021
Accepted December 22, 2021
Published online March 23, 2022

Corresponding Author
Yitao Jia
ORCID https://orcid.org/0000-0003-2610-9330
E-mail jiayitao99@163.com

Background/Aims: This study aimed to explore the effect of gut microbiota-regulated Kupffer cells (KCs) on colorectal cancer (CRC) liver metastasis.

Methods: A series of *in vivo* and *in vitro* researches were showed to demonstrate the gut microbiota and its possible mechanism in CRC liver metastasis.

Results: Fewer liver metastases were identified in the ampicillin-streptomycin-colistin and colistin groups. Increased proportions of *Parabacteroides goldsteinii*, *Bacteroides vulgatus*, *Bacteroides thetaiotaomicron*, and *Bacteroides uniformis* were observed in the colistin group. The significant expansion of KCs was identified in the ampicillin-streptomycin-colistin and colistin groups. *B. vulgatus* levels were positively correlated with KC levels. More liver metastases were observed in the vancomycin group. An increased abundance of *Parabacteroides distasonis* and *Proteus mirabilis* and an obvious reduction of KCs were noted in the vancomycin group. *P. mirabilis* levels were negatively related to KC levels. The number of liver metastatic nodules was increased in the *P. mirabilis* group and decreased in the *B. vulgatus* group. The number of KCs decreased in the *P. mirabilis* group and increased in the *B. vulgatus* group. *In vitro*, as *P. mirabilis* or *B. vulgatus* doses increased, there was an opposite effect on KC proliferation in dose- and time-dependent manners. *P. mirabilis* induced CT26 cell migration by controlling KC proliferation, whereas *B. vulgatus* prevented this migration.

Conclusions: An increased abundance of *P. mirabilis* and decreased amount of *B. vulgatus* play key roles in CRC liver metastasis, which might be related to KC reductions in the liver. **(Gut Liver 2022;16:575-588)**

Key Words: Colorectal neoplasms; Liver metastasis; Gastrointestinal microbiome; Kupffer cells

INTRODUCTION

Globally, the most prevalent type of malignant tumor is colorectal cancer (CRC),[1] and many of the CRC patients (15% to 25%) are diagnosed with metastasis of cancer.[2] Despite advancements in the therapeutic strategies of CRC liver metastasis, there is a huge population of patients (>50%) who experience recurrence and metastasis of cancer within 2 years.[3] Therefore, exploring the mechanism involved in the CRC liver metastasis is critical in improving the treatment options.

The cancer metastasis is associated with the cancer microenvironment *in situ* as well as in target organs, which can result in remarkable differences in the prognosis even for a similar stage of tumor.[4] There is an amazing connection between the gut and the liver homeostasis is influenced by the alterations in the CRC microenvironment through the gut-liver axis.[5] The CRC microenvironment is immensely complicated and consisted of the intestinal microbiota along with its products/metabolites.[6] Particu-

larly, any alterations in the gut microflora have a significant role in the CRC microenvironment affecting the development and recurrence of CRC. It has been observed that decreased *Bacteroides* and increased *Clostridial* populations promote CRC liver metastasis.[7] Additionally, several types of bacteria from the intestinal microflora can be introduced into the portal circulation of the liver by the microbe-associated molecular patterns, in this way improving the liver microenvironment.[8]

Although intestinal microbiota conciliate the hepatic natural killer T cell accumulation with both primary hepatic cancer and metastatic hepatic cancers, the possible alterations in the Kupffer cells (KCs), the most copious residential macrophages in the sinusoids of liver, have not been evaluated.[9] Among all hepatic non-parenchymal cells in the liver, KCs makeup up 20% of these and have a significant role in tumor phagocytosis.[10] KCs regulate the function and activity of the T-cells and natural killer (NK) cells. KCs stimulate the NK cells to produce and secrete the cytokines, for example, granulocyte-macrophage colony-stimulating factor and interferon-γ, that increases the pathogenicity of the KCs.[11] It has also been observed that the KCs influence the multiplication of the stimulated CD8+ T-cells during the initial stages of cancer and enhance the apoptosis in the later stages of cancer.[12] Several animals studies have proposed that the KCs increase the apoptosis of T-cell via Fas/Fas-L pathway and express the upper levels of programmed death-ligand 1 to obstruct multiplication and functionality of the T-cells by direct contact.[13,14] Therefore, the KCs have a complicated role in tumor progression.

KCs are involved in the killing of microbes by phagocytosis that invades from the bloodstream; so killing the *Borrelia burgdorferi* that expresses the green fluorescent protein and then presents the antigens to NK cells.[15] Lactic acid produced by the bacteria controls the KCs by lowering the lipopolysaccharide levels in the serum, alleviating the formation of non-alcoholic steatohepatitis.[16] The lipopolysaccharide is an inflammatory signal activating the Toll-like receptors on KCs thus ultimately causing the inflammation in the alcoholic liver disease.[17] A few studies are present regarding the influence of intestinal microflora on the KCs in CRC liver metastasis. The present study was designed to evaluate the role of intestinal microbiome and KCs in CRC liver metastasis, and to provide bass for devising the treatment and prevention strategies.

MATERIALS AND METHODS

1. Bacteria and cell culture

The mice colon tumor cell line colon 26 (CT26; Cell Bank of the Chinese Academy of Sciences, Shanghai, China) and hepatic KC cell line (Guangzhou Jennio Biotech Co., Ltd., Guangzhou, China) were cultured in Roswell Park Memorial Institute 1640 (Gibco, Santa Cruz, CA, USA) complete 10% fetal bovine serum (FBS; Gibco) supplemented medium and having 1% streptomycin along with 1% penicillin (Gibco) at 37℃ in a CO_2 (5%) incubator.[18] *Proteus mirabilis* (BNCC® 107943) and *Bacteroides vulgatus* (BNCC® 337471) were obtained from the Bena Culture Collection, Xinyang, China. *P. mirabilis* was grown on Columbia blood agar plates, and *B. vulgatus* was cultivated in Gifu Anaerobic Medium Broth (KisanBio, Seoul, Korea) in a 2.5 L Round Bottom Vertical Anaerobic Culture Bag (Qingdao Hope Bio-Technology Co., Ltd., Qingdao, China) and AnaeroPack®-Anaero (Mitsubishi Gas Chemical, Inc., Tokyo, Japan) at 37℃. All anaerobic culture media were deoxygenated for at least 24 hours prior to use.

2. Animal experiments

In this study, 6 weeks old, 60 male BALB/c specific-pathogen-free mice (Animal Experiment Center of Hebei Medical University, Shijiazhuang, Hebei, China) were used and differentiated into four random groups, each group having 15 mice. Antibiotics were administered in sterile drinking water to each group as per the following tab: administrated in sterile drinking water to control group (without antibiotics); vancomycin (Vanc) group (0.25 mg/mL vancomycin); colistin (Coli) group (2 mg/mL colistin); ampicillin-streptomycin-colistin (ASC) group (1 mg/mL ampicillin, 5 mg/mL streptomycin and 1 mg/mL colistin) (Table 1).[19]

Fecal sample collection was done 2 weeks after the antibiotic treatment and later 16S rDNA sequencing was done. The antimicrobial effects of antibiotics, used in this study, were observed and a model of CRC liver metastasis was made via splenic inoculation of CT26 cells (1×10^5) as mentioned earlier (Fig. 1A).[20]

Table 1. Groups of Mice with Antibiotic Protocols[19]

Group	Treatment
Control group	No antibiotics
Vanc group	Vancomycin (0.25 mg/mL)
Coli group	Colistin (2 mg/mL)
ASC group	Ampicillin (1 mg/mL) Streptomycin (5 mg/mL) Colistin (1 mg/mL)

Fifty-six specific-pathogen-free male BALB/c mice (aged 6 weeks) were bred in the specific-pathogen-free Laboratory Animal Center of Hebei General Hospital. Before the experiment, antibiotics were administered to mice of all groups through sterile drinking water containing 0.2 g/L ampicillin, neomycin, and metronidazole and 0.1 g/L vancomycin daily for 2 weeks.[21] Then, mice were divided into seven groups (n=8) based on intragastric gavage twice weekly with 2×10^8 colony-forming units (CFU)/0.2 mL *P. mirabilis* or heat-killed *P. mirabilis*, 2×10^8 CFU/0.2 mL *B. vulgatus* or heat-killed *B. vulgatus*, 1×10^8 CFU/0.1 mL *P. mirabilis* and 1×10^8 CFU/0.1 mL *B. vulgatus* or 1×10^8 CFU/0.1 mL heat-killed *P. mirabilis* and 1×10^8 CFU/0.1 mL heat-killed *B. vulgatus*, and 0.2 mL stroke-physiological saline solution (control group).[22] After 1 week of *P. mirabilis* and *B. vulgatus* administration, a CRC liver metastasis model was established and we continued to administer *P. mirabilis* or *B. vulgatus* via gavage until the end of experiment. This study was approved by the Administration Committee of Experimental Animals, Hebei General Hospital, Hebei Province, China (approval number: SYXK(Ji)-2020-005).

3. Bacterial 16S rDNA sequencing

Mice fecal pellets were collected and gene sequencing of 16S rDNA was done before making the CT26 tumor-bearing model. The 16S rDNA was done following the evaluation of antibacterial effect in groups.

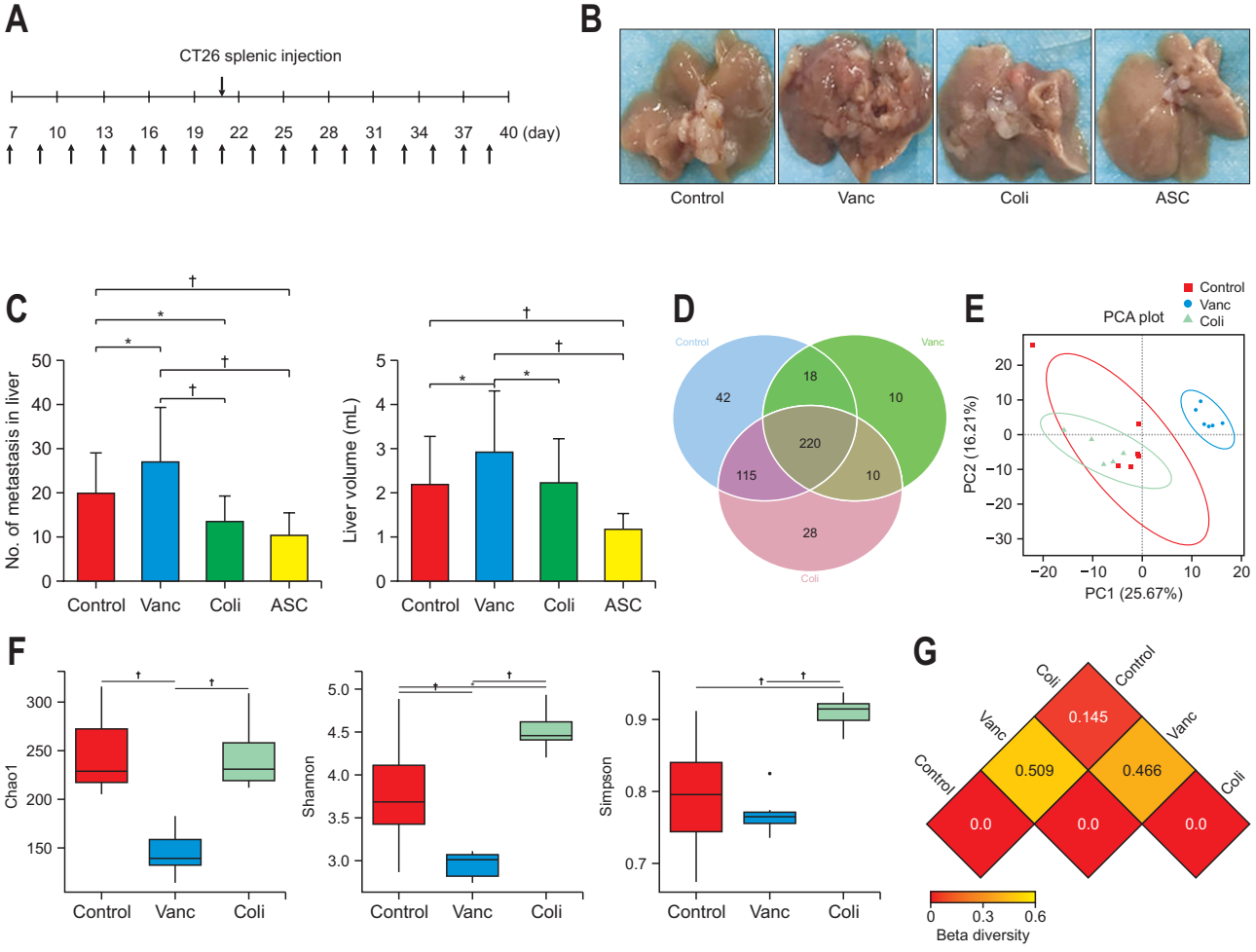

Fig. 1. Changes in gut microbiota and colorectal cancer (CRC) liver metastasis induced by different antibiotics. (A) Schematic diagram of the mouse experimental process of CRC liver metastasis with different antibiotics (upper arrow: CRC liver metastasis model, as established by colon 26 [CT26] splenic injection; lower arrow: antibiotic treatment). (B) Image of CRC liver metastases in animals treated with different antibiotics at the end of the experiment. (C) Number of CRC liver metastases and liver volume in different groups (n=15 per group; a mouse in the Vanc group and a mouse in the ASC group were lost during the experiment due to emaciation and intestinal obstruction). (D) Venn diagram of the total number of species among the control, Vanc, and Coli groups (n=6 per group). (E) Principal coordinates analysis (PCA) of operational taxonomic units in the control, Vanc, and Coli groups. (F) Alpha diversity analysis of the gut microbiomes among the control, Vanc, and Coli groups. Alpha diversity includes the Shannon, Chao1, and Simpson indices. (G) Beta diversity, reflected by the weighted Unifrac distance.
Control group, untreated; Vanc group, vancomycin; Coli group, colistin; ASC group, a mix of ampicillin, colistin and streptomycin. *p<0.05, †p<0.01.

The extraction of DNA was done from fecal samples by the cetyltrimethylammonium bromide (Sigma-Aldrich, St. Louis, Mo, USA) method. Agarose gel electrophoresis was utilized to detect the concentration and purity of DNA extracted from the fecal samples of mice. A suitable quantity of DNA was taken in a centrifuge tube and dilution was made up to 1 ng/μL in sterile water, then primer sequence 806R (5'-GGA CTA CNN GGG TAT CTA AT-3') and 515F (5'-GTG CCA GCM GCC GCG GTA A-3') were used to amplify the V3-V4 regions by polymerase chain reaction.

The DNA library was developed with the Ion Plus Fragment Library Kit (48 reactions; Thermo Fisher Scientific, Waltham, MA, USA). This developed DNA library was quantified by a Qubit (Thermo Fisher Scientific) as well as sequenced with an Ion S5TMXL (Thermo Fisher Scientific). Then the comparison of the reading sequence was done with the species annotation database Aby (https://github.com/torognes/vsearch/) along with the examination of chimera sequences. Clean reads were left only after the removal of the chimera sequence. Clustering was done with Uparse software (Uparse v7.0.1001, https://drive5.com/uparse/) with 97% similarity, and the operational taxonomic units regarding the species categorization were acquired following chimera filtering the clustered sequence.

The filter value was defined by the linear discriminant analysis effect size software and it was 4. Following the assurance of the operational taxonomic unit annotation data from the SILVA database (SILVA SSU 138.1, https://www.arb-silva.de), the entire information of the functional genomic for the prokaryotes in the Kyoto Encyclopedia of Genes and Genomes database was interpreted through UProC, and then by using the DNA aligner, the proteins were aligned in association with the SILVA database, in this way the functional prediction of Tax4Fun was perceived.

4. Immunohistochemistry (IHC)

The liver samples from mice were collected, fixed, impregnated, and embedded in paraffin wax, and sections were made (4 μm). A monoclonal rabbit anti-mouse F4/80 primary antibody (1:500; Servicebio, Wuhan, China) was added to the sections following the dewaxing & hydrating the sample, antigen repair, and 15 minutes incubating in H_2O_2 solution (3%). A 3,3'-diaminobenzidine staining solution IHC kit (Zsbio, Beijing, China) was used for color development. Three high-power microscopic fields were selected randomly and micrographs were taken with the microscope (Nikon, Tokyo, Japan). Image J (Ver-1.8.0, National Institutes of Health, Bethesda, MD, USA) was used to calculate the optical densities of proteins.

5. KC proliferation

KCs were cultured in tissue plates with 96 wells and these were used as at 5×10^3 cells in each well, then allowed to settle and adhere. Grown to late-log phase in 1640 complete medium supplemented with 10% FBS, *P. mirabilis* or *B. vulgatus* was separately added at concentrations of 1×10^3, 1×10^4, 1×10^5, 1×10^6, and 1×10^7 CFU/mL, and six wells were used for each group. After 12, 24, 48, and 72 hours incubation at 37℃, and Cell Counting Kit-8 (CCK8; Dojindo, Kumamoto, Japan) was used to count the cell numbers that were viable.

6. CT 26 cell migration

KCs (1×10^5) were inoculated on 24-well plates (lower chamber) with 500 μL 1640 medium and cultured for 24 hours; 50 μL of phosphate-buffered saline, 1×10^3, 1×10^4, 1×10^5, 1×10^6, or 1×10^7 CFU/mL *P. mirabilis* or *B. vulgatus* were added into the lower chamber and cultured for 24 hours (37℃, 5% CO_2). Then, culture medium was removed and 500 μL 1640 medium containing 20% FBS was added to the lower chamber. CT26 cells (5×10^4) in 100 μL 1640 medium with no FBS were added to the upper chamber, which was gently moved into the lower chamber and cocultured for 24 hours. The upper chamber was removed and rinsed with phosphate-buffered saline, fixed for 15 minutes with paraformaldehyde (4%) at room temperature, and then staining was done at 37℃ by using 0.1% crystal violet for 30 minutes. After that three fields were randomly selected under an inverted microscope to assess the cellular migration ability in each group (n=3). The number of CT26 cells passing via the Transwell supraventricular membrane was calculated with ImageJ software.

7. Statistical analysis

The data, from this study, were analyzed with SPSS software SPSS version 19.0 (IBM Corp., Armonk, NY, USA) and the data are expressed as the mean±standard deviation. Limited slip differential and one-way analysis of variance were utilized for multiple comparisons after testing the variance homogeneity and normal distribution of data. The correlation between differential bacteria and KCs were analyzed by using the Pearson correlation analysis between the Vanc group, Coli group, and control group. The differences of intestinal microbiome between different groups were statistically investigated by R software (R Foundation for Statistical Computing, Vienna, Austria). The comparisons of more than two groups were done with the Wilcoxon tests and the Tukey *post hoc* test by using the Agricola package and comparisons of two groups were done with the Wilcoxon rank-sum tests and the Student t-tests. The level of significance was kept at 5% ($p<0.05$).

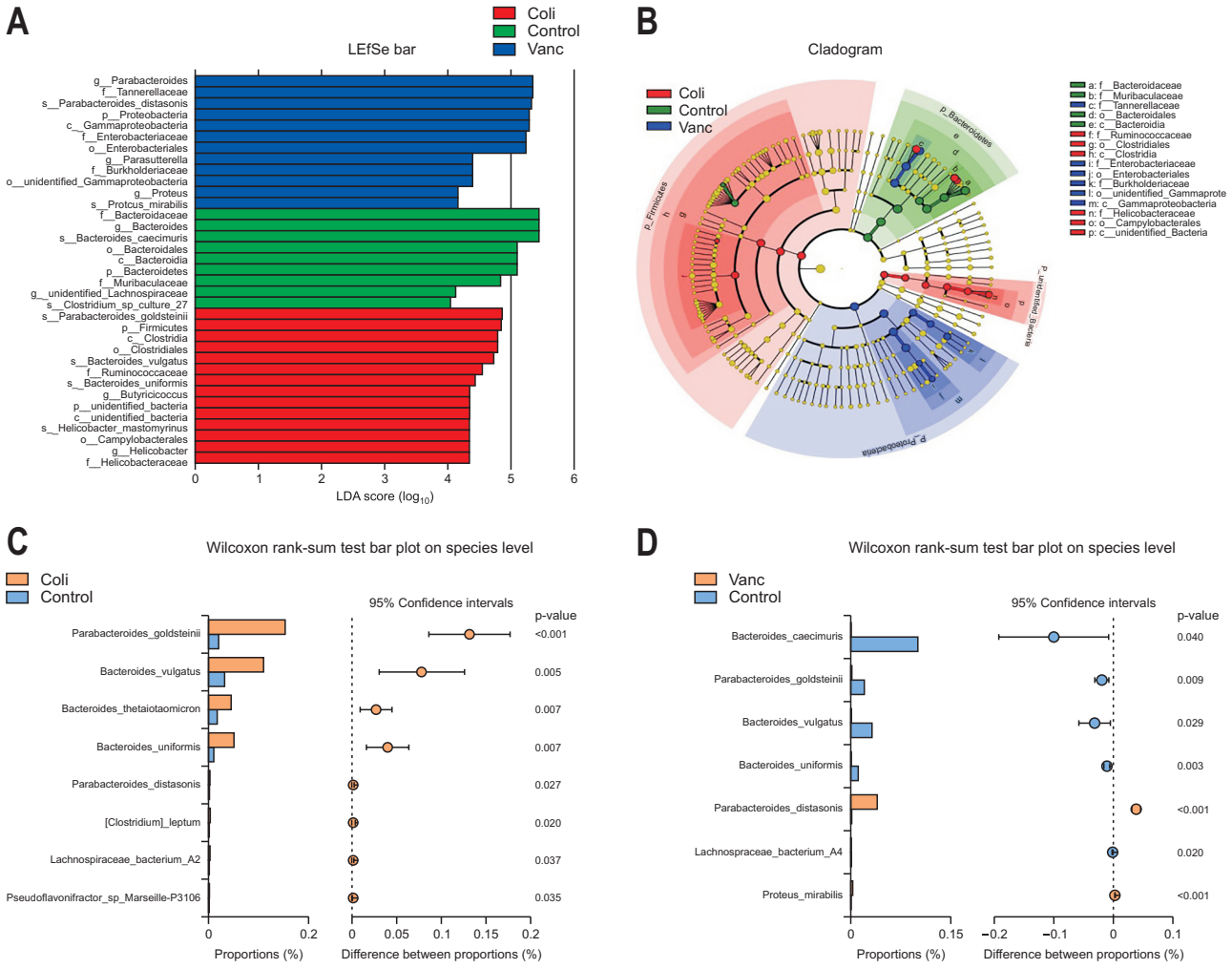

Fig. 2. Comparison of gut microbiota composition among three groups. (A) Linear discriminant analysis effect size (LEfSe) for differentially abundant taxa from the three groups. p=0.05 using the Wilcoxon rank-sum test, with linear discriminant analysis (LDA) score >4. (B) Taxonomic cladogram from the LEfSe showing differences in fecal taxa. Dot sizes are proportional to the abundance of the taxon (n=6 per group). (C) Compositional differences at the species level in the gut microbiome between the control and Coli groups. (D) Compositional differences at the species level in the gut microbiome between the control and Vanc groups.
Control group, untreated; Vanc group, vancomycin; Coli group, colistin; ASC group, a mix of ampicillin, colistin, and streptomycin.

RESULTS

1. Effect of alterations in the gut microbiota on CRC liver metastasis

The splenic tumor injection resulted in sudden CRC liver metastasis in BALB/c mice as mentioned earlier (Fig. 1A).[9] In the ASC group, antibiotics mixed in drinking water affected the intestinal commensal population negatively (Fig. 1B).[23] Fewer liver metastases were observed in the ASC group (p=0.003). Vancomycin promoted the CRC liver metastases (p=0.028) while colistin inhibited the CRC liver metastases (p=0.041). Vancomycin-treated mice group targeting the Gram-positive bacteria showed greater (p<0.001) liver metastases than the colistin-treated group of mice targeting the Gram-negative bacteria; comparing with this, a vigorous decrease (p<0.001) was identified in the liver metastasis in ASC group as compared to Vanc group. In this experiment, the liver volume showed identical results; liver volume was larger (p=0.028) in the Vanc group but it was in the ASC group, the liver volume was smaller (p=0.009). Furthermore, liver volume was greater (p=0.037) in the Vanc group as compared to the ASC group and Coli group (Fig. 1B and C).

To better understand the part of intestinal microbiome in response to the CRC liver metastasis, six fecal samples were collected from each group including the Coli, Vanc, ASC, and control groups, and 16S rDNA sequencing was done to assess the microbiota landscape in the fecal samples. Among all treatment groups, ASC treatment showed significant effects on intestinal commensal bacteria by

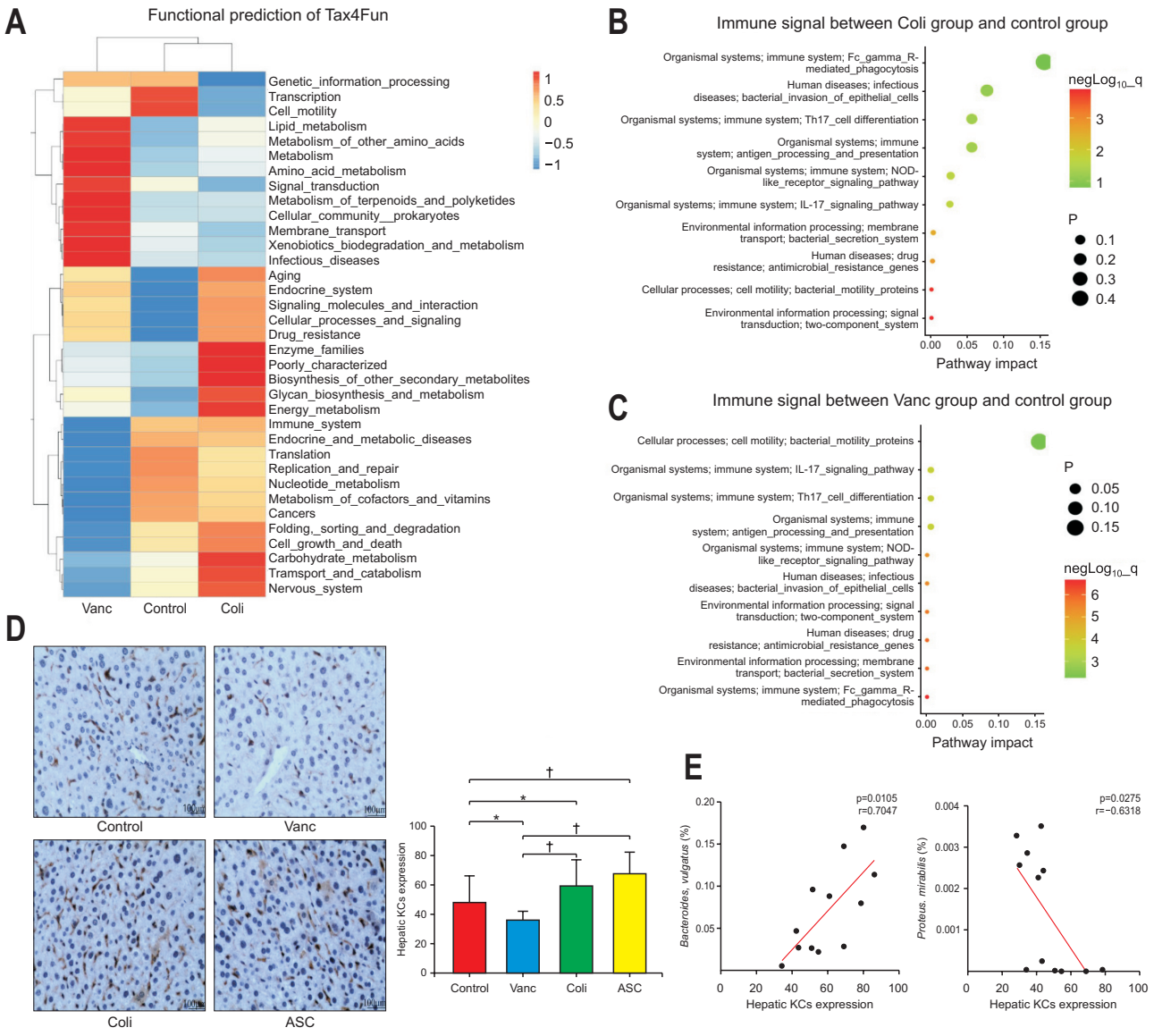

Fig. 3. Tax4Fun functional prediction analysis of differential bacteria associated with hepatic Kupffer cell (KC) accumulation; tumor inhibition was noted in the three groups. (A) Tax4Fun functional prediction in the control, Vanc, and Coli groups, as shown as a heatmap. (B) Enrichment of immune system, environmental information, and cellular process pathways were compared in the control and Coli groups (dot size symbolizes the p-value). (C) Enrichment of immune system, environmental information, and cellular process pathways were compared in the control and Vanc groups. (D) Hematoxylin and eosin staining images and quantification of hepatic KCs from different gut flora backgrounds (n=5 per group, ×200). (E) Analysis of the correlation between KCs and *Proteus mirabilis* or *Bacteroides vulgatus*.
Control group, untreated; Vanc group, vancomycin; Coli group, colistin; ASC group, a mix of ampicillin, colistin, and streptomycin. *p<0.05, †p<0.01.

eliminating them from the intestines. A Venn diagram graph showed that 220 species of bacteria were common among all species identified from the control group (n=395), Vanc group (n=258), and Coli group (n=373) in this study (Fig. 1D). According to the principal coordinate analysis, the microbial population structure was visibly different between the Coli group and Vanc groups, while there was no clear separation between control group and Coli group (Fig. 1E). Additionally, the alpha diversity of the intestinal microbiome was significantly different between Vanc group and Coli group which was observed by certain methods including Shannon, Chao1, and Simpson; moreover, a remarkable elevation in the microbial diversity of the Coli group was observed by Simpson and Shannon diversity (Fig. 1F). According to the beta diversity analysis, the different coefficients of intestinal microbiota diversity in the Vanc group and the Coli group were 0.509 and 0.145, respectively. Moreover, the correlation coefficient of commensal bacteria between the Vanc group and the Coli group was 0.466 (Fig. 1G). These results of this study sug-

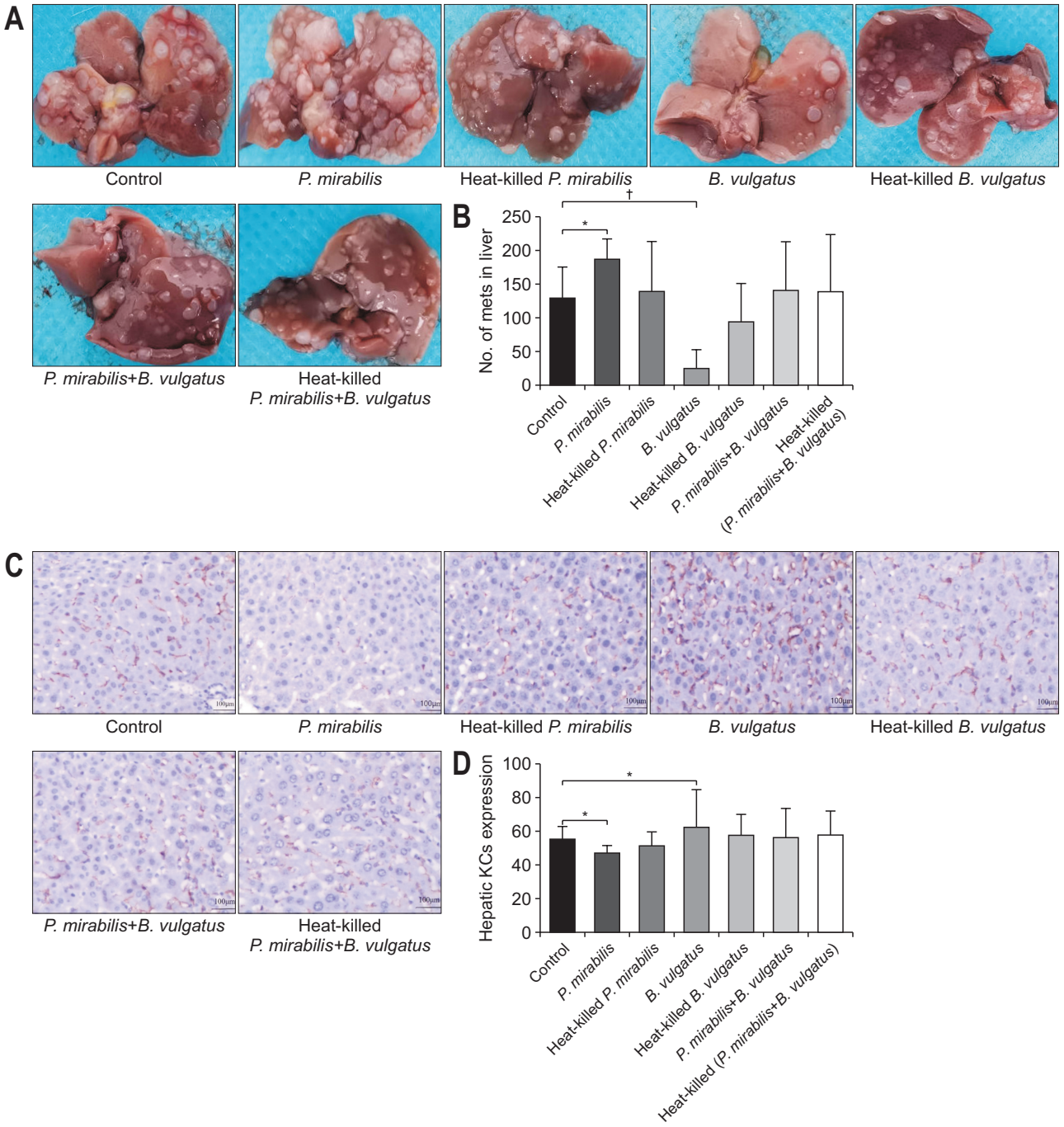

Fig. 4. Colorectal cancer (CRC) liver metastasis and hepatic Kupffer cell (KC) induced by *Proteus mirabilis* or *Bacteroides vulgatus*. (A) Images of liver metastatic nodules in each group. (B) Numbers of liver metastases in each group. Hematoxylin and eosin staining images (×200) (C) and quantification of hepatic KCs from different bacteria treatment (D).
Control group, untreated; Vanc group, vancomycin; Coli group, colistin; ASC group, a mix of ampicillin, colistin, and streptomycin. *p<0.05, †p<0.01.

gested the fact that modulating the intestinal commensal bacteria influenced the CRC liver metastasis in a way that the increased diversity and community richness might suppress the CRC liver metastasis.

2. Specificity of intestinal microbiota in CRC liver metastasis

In this study, the disagreement between the intestinal microbiome of all three groups were evaluated and high-dimensional class comparisons regarding the common taxa of intestinal bacteria were determined via linear discriminant analysis effect size bar and cladogram

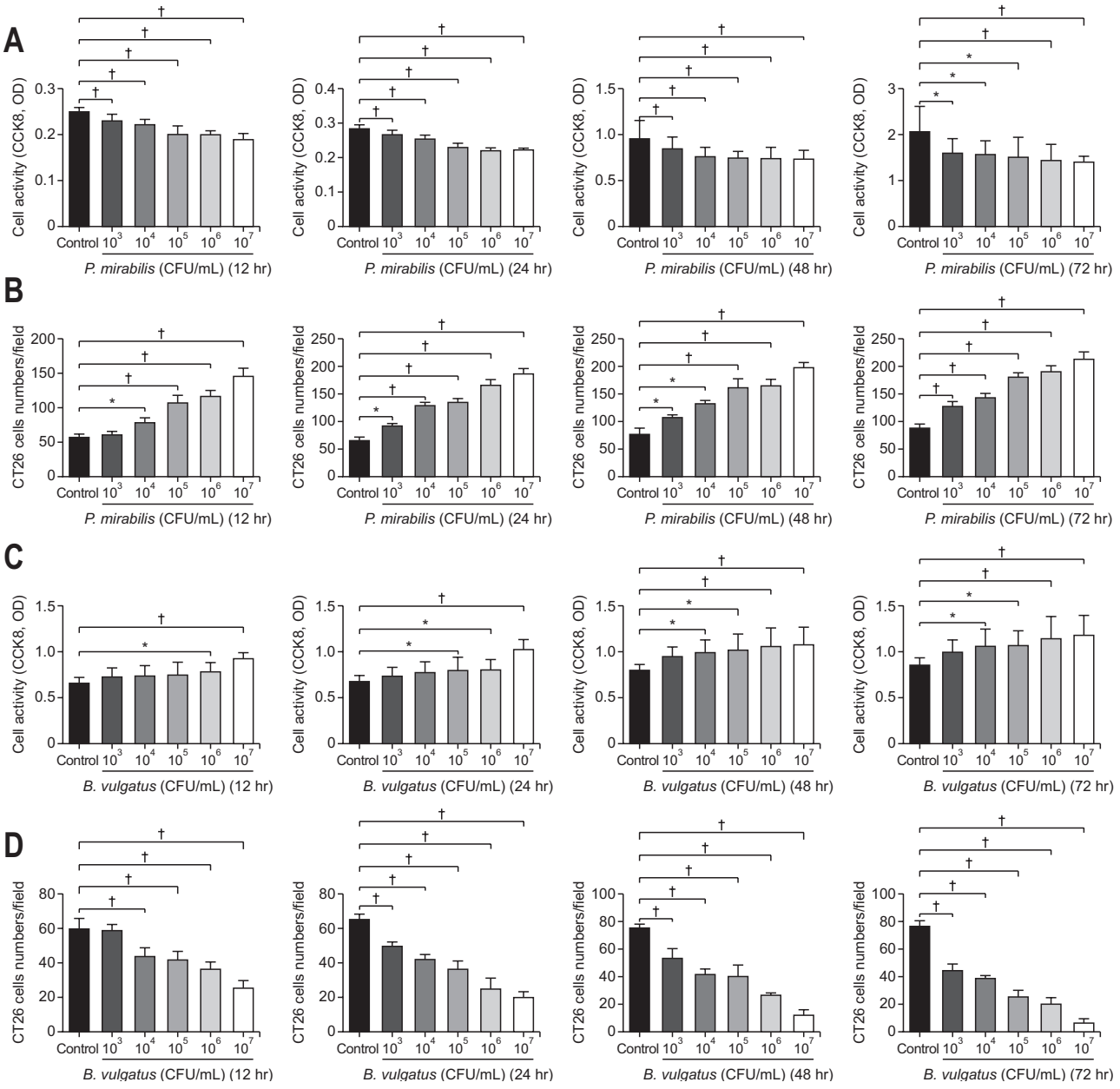

Fig. 5. Differential influences of *Proteus mirabilis* or *Bacteroides vulgatus* on Kupffer cell (KC) proliferation and effects of KCs induced by *P. mirabilis* or *B. vulgatus* on CT26 cell migration. (A) The difference in KC proliferation between the 10^3, 10^4, 10^5, 10^6, and 10^7 CFU/mL *P. mirabilis* groups and phosphate-buffered saline (PBS) group. (B) Migration of CT26 cells induced by KCs treated with different doses of *P. mirabilis* (n=3 per group). (C) Differences in KC proliferation between 10^3, 10^4, 10^5, 10^6, and 10^7 CFU/mL *B. vulgatus* groups and the PBS group. (D) Migration of CT26 cells induced by KCs treated with different doses of *B. vulgatus* (n=3 per group).
CFU, colony-forming unit. *p<0.05, †p<0.01.

analysis. The Coli group had abundant Bacteroidetes and Firmicutes; while the Vanc group had abundant Proteobacteria, considering the phylum level. Additionally for the species levels, the Coli group was found to be rich with *Helicobacter mastomyrinus*, *Bacteroides uniformis*, and *B. vulgatus* while the Vanc group was rich with *P. mirabilis* (Fig. 2A and B). Having similarity with the control group, according to the Wilcoxon rank-sum test, the Coli group had increased communities of *Bacteroides thetaiotaomicron*, *Parabacteroides goldsteinii*, *B. uniformis*, and *B. vulgatus*, while Vanc group was enriched with *P. mirabilis* and *Parabacteroides distasonis* (p<0.05) (Fig. 2C and D). These results of the current study suggested that the elevated populations of *P. mirabilis* and *P. distasonis* might favor the CRC liver metastasis and the elevated populations of *B. uniformis*, *P. goldsteinii*, *B. thetaiotaomicron*, and *B. vulga-*

tus could restrict the CRC liver metastasis.

3. Functional prediction of differential bacteria among groups

The functional prediction was done with Tax4Fun to assess the mechanism for the role of commensal bacteria in causing liver metastasis. The differential gene functions in all three groups contained the genes, immune system, cell motility, transport, and various types of metabolism (Fig. 3A). To detect the difference in immune responses, pairwise comparisons were done, which revealed that clear differences were observed in the immune system between the control group and Vanc group and between control and Coli groups. These differential functions between the three groups consisted of bacterial secretion system, NOD-like receptor signaling, bacterial motility protein, interleukin (IL)-17 signaling, and two-component system (Fig. 3B and C, Supplementary Fig. 1A). This suggested that the alterations in the intestinal microbiota influenced the CRC liver metastasis and it was associated with the IL-17 signaling.

4. Role of hepatic KCs in CRC liver metastasis and its co-relationship with differential microbiota

Based on the Tax4Fun prediction data, the immune signals particularly the IL-17, were clearly different between all the three groups. IHC was used to detect the count of KCs count in CT26 cancer-bearing mice, to evaluate the mechanism involved in the tumor suppression. The KCs were significantly high in the Coli and ASC groups (p=0.038, p=0.001, respectively), whereas the KCs were significantly less (p=0.027) in the Vanc group. There was a similarity in the KCs number with liver volume and liver metastasis results that the KCs were more in the mice of Coli group and ASC group as compared to that in the Vanc group (p<0.001, p<0.001, respectively) (Fig. 3D).

The results here highlighted the KC landscape of CRC liver metastasis and the huge remodeling after gut microbiota alterations.

The relation of KCs and differential count of bacteria were evaluated to detect the definitive role of the intestinal microbiome in regulating hepatic KC accumulation. A positive was found between KC contents and *B. vulgatus* (p=0.011, r=0.705), while a negative correlation was found between the KC contents and *P. mirabilis* (p=0.028, r=0.632) (Fig. 3E, Supplementary Fig. 1B and C). Hepatic KC count might be affected by increased *B. vulgatus* and decreased of *P. mirabilis* populations together, yielding in altered CRC liver metastasis tendencies.

5. *P. mirabilis* or *B. vulgatus* affects liver metastases in tumor-bearing mice

To validate the effect of *P. mirabilis* or *B. vulgatus* on liver metastasis, we counted liver metastatic nodules in tumor-bearing mice after *P. mirabilis* or *B. vulgatus* administration. *In vivo*, the numbers of liver metastases in the control, *P. mirabilis*, and heat-killed *P. mirabilis* groups were 130.8±44.6, 190.3±29.8, and 141.6±71.8, respectively, with a significant difference between *P. mirabilis* and control groups (p=0.046). In contrast, the numbers of liver metastases in the control, *B. vulgatus*, and heat-killed *B. vulgatus* groups were 130.8±44.6, 27.8±25.9, and 95.8±56.2, respectively, with a significant different between *B. vulgatus* and control groups (p=0.001). Heat-killed *P. mirabilis* or *B. vulgatus* treatment, as well as a combination of *P. mirabilis* and *B. vulgatus* with or without sterilization, did not affect the growth of liver metastatic tumors in syngeneic BALB/c mice (Fig. 4A and B). These findings suggested that *P. mirabilis* or *B. vulgatus* could have a key role in CRC liver metastasis.

6. *P. mirabilis* or *B. vulgatus* treatment influences KC recruitment to liver metastatic microenvironment

Given the changes in hepatic KCs in CRC liver metastasis after antibiotic administration, we utilized IHC to estimate the KC content in the liver tissues of tumor-bearing mice pre-transplanted with *P. mirabilis* or *B. vulgatus*. It was shown that KCs were distributed in the surface of hepatic sinusoids. In accordance with our liver metastasis nodules data, the proportion of KCs was significantly lower in liver tissues of *P. mirabilis* group, while, the proportion of hepatic KCs obviously higher in *B. vulgatus* group as compared with the control group (p=0.037, p=0.047, respectively). The distribution of KCs was not different between the other groups and control group (Fig. 4C and D). Those data further confirmed that *P. mirabilis* or *B. vulgatus* could exert potential influence on KCs, which were proven to be effective against liver metastasis.

7. *P. mirabilis* or *B. vulgatus* affects CT26 cell migration by regulating KC proliferation

To pinpoint the relationship between *P. mirabilis* and KC changes, we analyzed the effects of *P. mirabilis* on KCs. *P. mirabilis* markedly inhibited KC proliferation relative to that in the control group at 12, 24, 48, and 72 hours (p<0.001, p<0.001, p=0.021, p=0.039, respectively) (Fig. 5A). The half maximal inhibitory doses ($LogIC_{50}$) of *P. mirabilis* at 12, 24, 48, and 72 hours were 4.013, 4.085, 2.988, and 2.481 CFU/mL, respectively. Next, we measured numbers of CT26 cells passing through Transwell membranes in each group. An increased number of CT26 cells was detected for *P. mirabilis* pretreated with KCs compared to

that in the group pretreated with phosphate-buffered saline (p<0.001, p<0.001, p<0.001, p<0.001, respectively) (Fig. 5C, Supplementary Fig. 2A). The $LogIC_{50}$ of *P. mirabilis*-induced KC-promoted CT26 cell migration at 12, 24, 48, and 72 hours was 4.700, 3.886, 3.986, and 4.105 CFU/mL, respectively. *P. mirabilis* affected KCs in dose- and time-dependent manners and further regulated CT26 cell migration.

Considering that *B. vulgatus* affected CRC liver metastasis *in vivo*, we determined whether the proliferation of KCs was induced by *B. vulgatus*. As shown in Fig. 5B, compared with that in the control group, KC proliferation increased remarkably with increasing doses of *B. vulgatus* (p<0.001, p<0.001, p<0.033, p<0.039, respectively). Intergroup comparisons showed that KC proliferation in the 10^7 and 10^6 *B. vulgatus* groups was higher as compared to the control group at 12 hours (p=0.020, p<0.001, respectively); similarly, KC proliferation in the 10^7, 10^6, and 10^5 *B. vulgatus* groups was increased at 24 hours (p=0.046, p=0.037, p<0.001, respectively), and KC proliferation in the 10^7, 10^6, 10^5, and 10^4 *B. vulgatus* groups was increased relative to that in the control group at 48 hours (p=0.031, p=0.014, p=0.005, p=0.003, respectively) and 72 hours (p=0.048, p=0.041, p=0.007, p=0.003, respectively). *B. vulgatus* treatment exerted pro-proliferative effects on KCs in dose- and time-dependent manners. The $LogIC_{50}$ of *B. vulgatus* at 12, 24, 48, and 72 hours was 6.384, 6.708, 2.863, and 3.113 CFU/mL, respectively. Moreover, *B. vulgatus* treatment ameliorated CT26 cell migration in dose- and time-dependent manners at 12, 24, 48, and 72 hours, with KC proliferation (p<0.001, p<0.001, p<0.001, p<0.001, respectively) (Fig. 5D, Supplementary Fig. 2B). The $LogIC_{50}$ of *B. vulgatus*-induced KC effects on CT26 cell migration at 12, 24, 48, and 72 hours was 3.990, 3.978, 3.378, and 3.055 CFU/mL, respectively.

To summarize, *P. mirabilis* appeared to exhaust the phagocytotic capacity of KCs and promoted CT26 cell migration; *B. vulgatus* potentially has an essential role in preventing CT26 cell migration in response to KC proliferation.

DISCUSSION

The mechanisms involved in CRC liver metastasis are unexplained yet. A recent theory of the gut-liver axis put forward the foundation for exploring the correlation between intestinal diseases and the liver. The hepatic portal venous system carries the microbiota into the liver that can bring changes in the liver microenvironment and may influence the CRC liver metastasis.[17] In the present study, different models of CRC liver metastasis were created by using different mouse-administered antibiotics. Comparatively, more liver metastasis was detected in the Vanc group comparing with those in the Coli group and mixed treatment group. It was also observed that the population of *P. mirabilis* was increased in the Vanc group and of *B. vulgatus* was found to be increased in the Coli group before metastasis. KCs can be related to the effect of intestinal microflora on CRC liver metastasis. Following this, we further proved that *P. mirabilis* favored CT26 cell migration and CRC liver metastasis by diminishing KC recruitment, whereas *B. vulgatus* controlled CT26 cell migration and CRC liver metastasis by increasing KC accumulation *in vitro* and *in vivo*.

The CRC hepatic metastasis modules were created in mice by various intestinal microflora. In the current study, the liver metastases were higher in the Vanc group as compared to the control group. Another study stated a remarkable decrease in the liver metastases in the Vanc group of mice.[9] This variation in the results can be due to different doses of antibiotic, treatment duration of antibiotic, feeding conditions of animals, selected strains of animals, or the number of cancerous cells inoculated through the spleen. Moreover, ASC group showed lesser liver metastases as compared to control group, which can be correlated with the depleted symbiotic bacteria in the intestine due to antibiotics. These results are in coordination with an earlier study by Sethi *et al.*[24] where they developed liver metastasis modules of melanoma, pancreatic cancer, and colon cancer in mice and used antibiotics to control the intestinal microflora. A cocktail of broad-spectrum antibiotics (metronidazole, amphotericin B, vancomycin, ampicillin, and neomycin) reduced the liver metastasis occurrence significantly. Liver metastases were increased in the control group as compared to that in the Coli group. Oral colistin administration causes a significant reduction in the fecal Gram-negative bacteria in a hepatic-induced mice model for colitis and lessened the systemic endo-toxemic damage in colitis.[25] Additionally, colistin can be used to treat the stubborn populations of *Escherichia coli* O157:H7 because the inoculation of *E. coli* via gastric route results in greater CRC tumors as well as increased metastases in CRC liver models.[26,27]

A definite separation in bacterial populations was noticed in three groups of mice as per the principal coordinate analysis, alpha diversity analysis, and beta diversity analysis of intestinal microflora. Many differences between the control group and the Vanc group and between the control group and the Coli group were analyzed for better identification of commensal bacterial populations responsible for CRC liver metastasis. Raised count of *P. mirabilis*

and *P. distasonis* might exaggerate the CRC liver metastasis, whereas raised counts of *B. uniformis*, *B. vulgaus*, *B. thetaiotaomicron*, and *P. goldsteinii* could restrict the CRC liver metastasis. Likewise, bacteria from genus Bacteroides, like *B. vulgatus*, have anti-cancerous effects that can be correlated with the immune response intervened by the activation of TLR2 signaling pathway and myeloid differentiation protein-2/TLR4.[28,29] T-cell responses specified for *B. fragilis* or *B. thetaiotaomicron* are connected with CTLA-4 blockade efficacy in cancer patients.[30]

The functional difference between the three mice groups was found to be correlated with immune signaling based on the prediction. Specifically, IL-17 promotes tumor progression that modulates the inflammatory responses in KCs according to an alcohol-induced hepatocellular carcinoma model.[31] The premetastatic niche development in the CRC liver metastasis comprises various cells, for example, cells of bone marrow origin and other resident cells like KCs, liver sinusoidal cells, and hepatic stellate cells. Among all these types of cells, KCs have an important role in CRC liver metastasis.[32] In the present study, having a similarity with the liver metastasis results, there was an increased population of KCs in the ASC group comparing with that in the control group which indicates that KCs aggregation was improved due to decreased commensal bacteria in the intestine. Significantly, it was observed that the KC population was reduced in the mouse of the Vanc group and increased in the mice of the Coli group.

Previous studies reported that vancomycin causes increase in IL-25 levels, *in vivo* and *in vitro*, and this elevated levels of IL-25 cause the stimulation of macrophages (M1 and M2 subtype alterations) which promotes the hepatocellular carcinoma growth.[33] A previous study stated that the colistin treatment might have positive influence on phagocytic capability of macrophages through p38/mitogen-activated protein kinase pathway.[34] Moreover, intrahepatic recurrence is more prevalent in patients with partial hepatectomy, it can be due to a decrease in the count of KCs residing in the liver which causes the activation of caspase 1, tumor necrosis factor α, and receptor-interacting protein kinase 3 to cause the recruitment of certain other monocyte-derived cells which are favorable for cancer growth.[35]

In the present study, in the Coli group KCs were abundant and these were significantly low in the Vanc group than in the control group indicating that CRC liver metastasis could be inhibited by the KC accumulation. Moreover, decreased *P. mirbilis* and increased *B. vulgatus* populations are positively associated with hepatic KCs encouraging that the *B. vulgatus* could be an important bacterium for KC aggregation. The neutrophil necrosis and macrophage accumulation were observed by light and electron microscopes following the inoculation of *B. vulgatus* and *T. hyodysenteriae* in mice.[36]

Changes in the liver microenvironment induced by commensal microbes could be beneficial for patients suffering from CRC liver metastasis. Here, more liver metastatic nodules were identified in the *P. mirabilis* group, but metastatic nodules were not increased in the heat-killed *P. mirabilis* group, suggesting that high relative abundances of *P. mirabilis* could increase metastasis, different from the results of a previous study.[37] These might be associated with the dose and method of *P. mirabilis* administration, the number of tumor cells injected, selection of animal strains, or animal feeding conditions. The characteristic aggregation of *P. mirabilis* within the cancerous can be used to transfer genes, immunomodulatory proteins, cytotoxic proteins, and prodrugs, showing similarity with *F. clostridium*.[38] In our study, *B. vulgatus* remarkedly inhibited CRC liver metastasis. This observation might indicate its protective effect on tumorigenesis, which has been suggested in several studies.[28,29] However, combined *P. mirabilis* and *B. vulgatus* had no effect on liver metastasis compared with the control group, showing that the efficacy of *B. vulgatus* might be counteracted by *P. mirabilis*.

Evidence has shown that several members of the intestinal microbiota, especially *P. mirabilis*, can be responsive to colitis in inflammatory macrophages, favoring IL-1β-dependent inflammation and intestinal damage.[39] *In vivo* and *in vitro*, our studies showed that *P. mirabilis* reduced KC recruitment and further promoted tumor metastasis and CT26 cell migration. It is well known that the 39 kDa protein of *P. mirabilis* can inhibit the LPS-induced oxidative response of macrophages in a dose-dependent manner.[40] Importantly, our recent studies also showed that the suppressive effect of *P. mirabilis* on KCs was dose- and time-dependent; when the dose of *P. mirabilis* was log 2.481 CFU/mL, the inhibitory effect was detected with cocultivation until 72 hours. In contrast, with an increasing dose to log 3.886 CFU/mL, *P. mirabilis* promoted CT26 cell migration through KCs at 24 hours, suggesting that an increase in the dose of *P. mirabilis* could accelerate CT26 cell migration after KC treatment at the early stage. Analogous to our Tax4Fun functional prediction based on 16S rDNA, *P. mirabilis* can translocate through the intestinal barrier and increase the proportion of T helper 17 cells, producing IL-17, to develop biliary disease and liver fibrosis.[41] Furthermore, *P. mirabilis* could reach the recruited inflammatory macrophages across the damaged epithelial layer, and the engulfed *P. mirabilis* strongly activate the NLRP3 inflammasome to induce robust IL-1β production, leading to the expansion of intestinal inflammation

and the formation of CRC.[42] Liver metastasis infiltrated by MRC1+CCL18+ M2-like macrophages shows higher phenylalanine metabolism, generating tyrosine, which could be linked to their unique functions at metastatic sites.[43]

Moreover, we found that *B. vulgatus* promoted KC accumulation *in vivo* and KC proliferation *in vitro* in dose- and time-dependent manners, preventing tumor metastasis and CT26 cell migration. *B. vulgatus* mpk, which provides only weak agonistic activity and leading to the improvement in the immune responses in a mouse colitis model.[44] Moreover *B. vulgatus*-induced IL-6 recruits dendritic cells towards an immature state where these cells do not respond to any pro-inflammatory activation by *E. coli*.[45] In our study, the proliferation of KCs was apparent until the dose of *B. vulgatus* was log 2.863 CFU/mL at 48 hours. When the concentration of *B. vulgatus* continued to log 3.055 CFU/mL, the proliferation of KCs inhibited CT26 cell migration at 72 hours, indicating that even if the dose of *B. vulgatus* increases, it takes certain amount of time to promote KC growth, which exerts anti-migration effects on CT26 cells. The ability of *B. vulgatus* to modulate NF-κB in HT-29 or Caco-2 cells is strain- and growth phase-dependent, suggesting that this capability might be regulated in response to environmental stressors affecting bacterial growth.[46]

However, the current study had certain limitations. In this study, one cell line (CT26) was utilized, the KC subtype was not recognized, and certain other cells of hepatic immune response were also not exposed. Moreover, the precise mechanism involved in the observed effects needs additional studies.

In conclusion, alterations to the gut microflora diversity influence CRC liver metastasis. An increased abundance of *B. vulgatus* and a decreased abundance of *P. mirabilis* can play key roles in CRC liver metastasis, which could be related to KC accumulation in the liver.

CONFLICTS OF INTEREST

No potential conflict of interest relevant to this article was reported.

ACKNOWLEDGEMENTS

This work was supported by The Specialist Capacity Building and Leader Development Program Funded from the 2018 Hebei Government (grant number: 361003).

The authors of this paper wish to pay regards to all who have contributed in writing this paper. We thank Dr. Li, the Department of General Surgery in the First Hospital of Hebei Medical University, for designing the study.

AUTHOR CONTRIBUTIONS

Concept and design: Z.L., Y.J. Data acquisition: N.Y., X.L., M.W., L.Q., Y.G. Data analysis and interpretation: N.Y., X.X., J.Z., Y.L. Drafting of the manuscript; critical revision of the manuscript for important intellectual content: N.Y., Z.L., Y.J. Statistical analysis: N.Y. Obtained funding: Y.J. Administrative, technical, or material support; study supervision: Z.L., Z.Z., Y.J. Approval of final manuscript: all authors.

ORCID

Na Yuan https://orcid.org/0000-0001-6268-6106
Xiaoyan Li https://orcid.org/0000-0001-8466-4135
Meng Wang https://orcid.org/0000-0002-4739-1884
Zhilin Zhang https://orcid.org/0000-0003-1976-2462
Lu Qiao https://orcid.org/0000-0003-1344-7859
Yamei Gao https://orcid.org/0000-0002-6913-538X
Xinjian Xu https://orcid.org/0000-0002-5138-5719
Jie Zhi https://orcid.org/0000-0003-1727-7746
Yang Li https://orcid.org/0000-0001-9245-6547
Zhongxin Li https://orcid.org/0000-0002-6375-1667
Yitao Jia https://orcid.org/0000-0003-2610-9330

SUPPLEMENTARY MATERIALS

Supplementary materials can be accessed at https://doi.org/10.5009/gnl210177.

REFERENCES

1. Kashyap D, Sharma A, Tuli HS, Sak K, Mukherjee T, Bishayee A. Molecular targets of celastrol in cancer: recent trends and advancements. Crit Rev Oncol Hematol 2018;128:70-81.
2. Lim CJ, Lee YH, Pan L, et al. Multidimensional analyses reveal distinct immune microenvironment in hepatitis B virus-related hepatocellular carcinoma. Gut 2019;68:916-927.
3. Imai K, Allard MA, Benitez CC, et al. Early recurrence after hepatectomy for colorectal liver metastases: what optimal definition and what predictive factors? Oncologist 2016;21:887-894.
4. Jia B. Commentary: gut microbiome-mediated bile acid metabolism regulates liver cancer via NKT cells. Front Im-

munol 2019;10:282.
5. Golonka RM, Vijay-Kumar M. Atypical immunometabolism and metabolic reprogramming in liver cancer: deciphering the role of gut microbiome. Adv Cancer Res 2021;149:171-255.
6. Kim SH, Lim YJ. The role of microbiome in colorectal carcinogenesis and its clinical potential as a target for cancer treatment. Intest Res 2022;20:31-42.
7. Li Y, Wang S, Sun Y, et al. Apple polysaccharide protects ICR mice against colitis associated colorectal cancer through the regulation of microbial dysbiosis. Carbohydr Polym 2020;230:115726.
8. Clarke TB, Davis KM, Lysenko ES, Zhou AY, Yu Y, Weiser JN. Recognition of peptidoglycan from the microbiota by Nod1 enhances systemic innate immunity. Nat Med 2010;16:228-231.
9. Ma C, Han M, Heinrich B, et al. Gut microbiome-mediated bile acid metabolism regulates liver cancer via NKT cells. Science 2018;360:eaan5931.
10. Huang H, Lu Y, Zhou T, Gu G, Xia Q. Innate immune cells in immune tolerance after liver transplantation. Front Immunol 2018;9:2401.
11. Kuniyasu Y, Marfani SM, Inayat IB, Sheikh SZ, Mehal WZ. Kupffer cells required for high affinity peptide-induced deletion, not retention, of activated CD8+ T cells by mouse liver. Hepatology 2004;39:1017-1027.
12. Tu Z, Bozorgzadeh A, Pierce RH, Kurtis J, Crispe IN, Orloff MS. TLR-dependent cross talk between human Kupffer cells and NK cells. J Exp Med 2008;205:233-244.
13. Chen Y, Liu Z, Liang S, et al. Role of Kupffer cells in the induction of tolerance of orthotopic liver transplantation in rats. Liver Transpl 2008;14:823-836.
14. Gong J, Cao D, Chen Y, Li J, Gong J, Zeng Z. Role of programmed death ligand 1 and Kupffer cell in immune regulation after orthotopic liver transplantation in rats. Int Immunopharmacol 2017;48:8-16.
15. Lee WY, Moriarty TJ, Wong CH, et al. An intravascular immune response to Borrelia burgdorferi involves Kupffer cells and iNKT cells. Nat Immunol 2010;11:295-302.
16. Okubo H, Kushiyama A, Sakoda H, et al. Involvement of resistin-like molecule β in the development of methionine-choline deficient diet-induced non-alcoholic steatohepatitis in mice. Sci Rep 2016;6:20157.
17. Ishida K, Kaji K, Sato S, et al. Sulforaphane ameliorates ethanol plus carbon tetrachloride-induced liver fibrosis in mice through the Nrf2-mediated antioxidant response and acetaldehyde metabolization with inhibition of the LPS/TLR4 signaling pathway. J Nutr Biochem 2021;89:108573.
18. Lai C, Li C, Liu M, et al. Effect of Kupffer cells depletion on ABC phenomenon induced by Kupffer cells-targeted liposomes. Asian J Pharm Sci 2019;14:455-464.
19. Lee JG, Lee YR, Lee AR, Park CH, Han DS, Eun CS. Role of the global gut microbial community in the development of colitis-associated cancer in a murine model. Biomed Pharmacother 2021;135:111206.
20. Eggert T, Wolter K, Ji J, et al. Distinct functions of senescence-associated immune responses in liver tumor surveillance and tumor progression. Cancer Cell 2016;30:533-547.
21. Wong SH, Zhao L, Zhang X, et al. Gavage of fecal samples from patients with colorectal cancer promotes intestinal carcinogenesis in germ-free and conventional mice. Gastroenterology 2017;153:1621-1633.
22. Qi X, Yun C, Sun L, et al. Gut microbiota-bile acid-interleukin-22 axis orchestrates polycystic ovary syndrome. Nat Med 2019;25:1225-1233.
23. Xu X, Lv J, Guo F, et al. Gut microbiome influences the efficacy of PD-1 antibody immunotherapy on MSS-type colorectal cancer via metabolic pathway. Front Microbiol 2020;11:814.
24. Sethi V, Kurtom S, Tarique M, et al. Gut microbiota promotes tumor growth in mice by modulating immune response. Gastroenterology 2018;155:33-37.
25. Gardiner KR, Erwin PJ, Anderson NH, McCaigue MD, Halliday MI, Rowlands BJ. Lactulose as an antiendotoxin in experimental colitis. Br J Surg 1995;82:469-472.
26. Percivalle E, Monzillo V, Pauletto A, Marone P, Imberti R. Colistin inhibits E. coli O157:H7 Shiga-like toxin release, binds endotoxins and protects Vero cells. New Microbiol 2016;39:119-123.
27. Li R, Zhou R, Wang H, et al. Gut microbiota-stimulated cathepsin K secretion mediates TLR4-dependent M2 macrophage polarization and promotes tumor metastasis in colorectal cancer. Cell Death Differ 2019;26:2447-2463.
28. Uronis JM, Mühlbauer M, Herfarth HH, Rubinas TC, Jones GS, Jobin C. Modulation of the intestinal microbiota alters colitis-associated colorectal cancer susceptibility. PLoS One 2009;4:e6026.
29. Di Lorenzo F, Pither MD, Martufi M, et al. Pairing Bacteroides vulgatus LPS structure with its immunomodulatory effects on human cellular models. ACS Cent Sci 2020;6:1602-1616.
30. Vétizou M, Pitt JM, Daillère R, et al. Anticancer immunotherapy by CTLA-4 blockade relies on the gut microbiota. Science 2015;350:1079-1084.
31. Ma HY, Yamamoto G, Xu J, et al. IL-17 signaling in steatotic hepatocytes and macrophages promotes hepatocellular carcinoma in alcohol-related liver disease. J Hepatol 2020;72:946-959.
32. Keirsse J, Van Damme H, Geeraerts X, Beschin A, Raes G, Van Ginderachter JA. The role of hepatic macrophages in liver metastasis. Cell Immunol 2018;330:202-215.
33. Li Q, Ma L, Shen S, et al. Intestinal dysbacteriosis-induced

IL-25 promotes development of HCC via alternative activation of macrophages in tumor microenvironment. J Exp Clin Cancer Res 2019;38:303.
34. Wang J, Shao W, Niu H, Yang T, Wang Y, Cai Y. Immunomodulatory effects of colistin on macrophages in rats by activating the p38/MAPK pathway. Front Pharmacol 2019;10:729.
35. Hastir JF, Delbauve S, Larbanoix L, et al. Hepatocarcinoma induces a tumor necrosis factor-dependent Kupffer cell death pathway that favors its proliferation upon partial hepatectomy. Front Oncol 2020;10:547013.
36. Albassam MA, Olander HJ, Thacker HL, Turek JJ. Electron microscopic studies on the interaction between normal mice peritoneal phagocytes and Treponema hyodysenteriae, Treponema innocens and Bacteroides vulgatus. Can J Vet Res 1986;50:88-95.
37. Zhang H, Diao H, Jia L, et al. Proteus mirabilis inhibits cancer growth and pulmonary metastasis in a mouse breast cancer model. PLoS One 2017;12:e0188960.
38. Heap JT, Theys J, Ehsaan M, et al. Spores of Clostridium engineered for clinical efficacy and safety cause regression and cure of tumors in vivo. Oncotarget 2014;5:1761-1769.
39. Seo SU, Kamada N, Muñoz-Planillo R, et al. Distinct commensals induce interleukin-1β via NLRP3 inflammasome in inflammatory monocytes to promote intestinal inflammation in response to injury. Immunity 2015;42:744-755.
40. Weber G, Heck D, Bartlett RR, Nixdorff K. Modulation of effects of lipopolysaccharide on macrophages by a major outer membrane protein of Proteus mirabilis as measured in a chemiluminescence assay. Infect Immun 1992;60:1069-1075.
41. Lemoinne S, Sabino J, Sokol H. Gut microbiota in PSC: from association to possible causality. Commentary to "Gut pathobionts underlie intestinal barrier dysfunction and liver T helper 17 cell immune response in primary sclerosing cholangitis" by Nakamoto et al., Nature Microbiology, January 2019. Clin Res Hepatol Gastroenterol 2020;44:123-125.
42. Chung IC, OuYang CN, Yuan SN, et al. Pretreatment with a heat-killed probiotic modulates the NLRP3 inflammasome and attenuates colitis-associated colorectal cancer in mice. Nutrients 2019;11:516.
43. Wu Y, Yang S, Ma J, et al. Spatiotemporal immune landscape of colorectal cancer liver metastasis at single-cell level. Cancer Discov 2022;12:134-153.
44. Steimle A, Michaelis L, Di Lorenzo F, et al. Weak agonistic LPS restores intestinal immune homeostasis. Mol Ther 2019;27:1974-1991.
45. Frick JS, Zahir N, Müller M, et al. Colitogenic and non-colitogenic commensal bacteria differentially trigger DC maturation and Th cell polarization: an important role for IL-6. Eur J Immunol 2006;36:1537-1547.
46. Ó Cuív P, de Wouters T, Giri R, et al. The gut bacterium and pathobiont Bacteroides vulgatus activates NF-κB in a human gut epithelial cell line in a strain and growth phase dependent manner. Anaerobe 2017;47:209-217.